

# Ets Domain Transcription Factor PE1 Suppresses Human Interstitial Collagenase Promoter Activity by Antagonizing Protein–DNA Interactions at a Critical AP1 Element<sup>†</sup>

Miri Bidder,<sup>‡,§</sup> Arleen P. Loewy,<sup>‡</sup> Tammy Latifi, Elizabeth P. Newberry, Glenda Ferguson, David M. Willis, and Dwight A. Towler<sup>\*,§</sup>

*Department of Molecular Biology and Pharmacology, Washington University School of Medicine, St. Louis, Missouri 63110*

*Received February 14, 2000; Revised Manuscript Received May 16, 2000*

**ABSTRACT:** In MC3T3E1 calvarial osteoblasts, fibroblast growth factor receptor (FGFR) signaling elicits multiple transcriptional responses, including upregulation of the interstitial collagenase/matrix metalloproteinase 1 (MMP1) promoter. FGF responsiveness maps to a bipartite Ets/AP1 element at base pairs –123 to –61 in the human MMP1 promoter. Under basal conditions, the MMP1 promoter is repressed in part via protein–DNA interactions at the Ets cognate, and minimally two mechanisms convey MMP1 promoter upregulation by FGF2: (a) transcriptional activation via Fra1/c-Jun containing DNA–protein interactions at the AP1 cognate and (b) derepression of promoter activity regulated by the Ets cognate. To identify osteoblast Ets repressors that potentially participate in gene expression in the osteoblast, we performed reverse transcription–polymerase chain reaction (RT-PCR) analysis of mRNA isolated from MC3T3E1 cells, using degenerative amplimers to the conserved Ets DNA binding domain to survey the Ets genes expressed by these cells. Six distinct Ets mRNAs were identified: Ets2, Fli1, GABPα, SAP1, Elk1, and PE1. Of these, only PE1 has extensive homology to the known Ras-regulated Ets transcriptional repressor, ERF. Therefore, we cloned and characterized PE1 cDNA from a mouse brain library and performed functional analysis of this particular Ets family member. A 2 kb transcript was isolated from brain that encodes a ~57 kDa protein; the predicted protein contains the known N-terminal Ets domain of PE1 and a novel C-terminal domain with significant homology to murine ERF. The murine PE1 open reading frame (ORF) is much larger than the previously reported human PE1 ORF. Consistent with this, affinity-purified rabbit anti-mouse PE1 antibody specifically recognizes an ~66 kDa protein present only in the nuclear fraction of MC3T3E1 osteoblasts. Recombinant PE1 binds authentic AGGAWG Ets DNA cognates, and transient transfection studies demonstrate that PE1 represses MMP1 promoter activity. Surprisingly, although deletion of the MMP1 Ets cognate at nucleotides –88 to –83 abrogates FGF2 induction, it does not prevent suppression of the AP1-dependent MMP1 promoter by PE1. PE1 regulation maps to the MMP1 promoter region –75 to –61, suggesting that PE1 suppresses transcription via protein–protein interactions with AP1. Consistent with this, recombinant GST–PE1 specifically inhibits the formation of protein–DNA interactions on the MMP1 AP1 site (–72 to –66) when present in an admixture with MC3T3E1 crude nuclear extract. In toto, these data indicate that PE1 participates in the transcriptional regulation of the MMP1 promoter in osteoblasts. As observed with other transcriptional repressors of MMP1 gene expression, transcriptional suppression by PE1 occurs via inhibition of AP1-dependent promoter activity.

The Ets domain family is a large and biologically diverse collection of transcription factors that control stage- and tissue-specific gene expression in higher eukaryotes (1). Ets domain proteins function primarily as transcriptional co-regulators that have relatively low intrinsic transactivation

function (1). Although transactivation function has been identified in a few Ets proteins (2, 3), upregulation of gene expression by Ets domain factors depends in great measure upon cooperative interactions with potent transactivators that bind to nearby cis elements (1, 4). These collaborative factors have generally been identified as members of the leucine zipper family (e.g., Myb, AP1, C/EBP) (5–7) but also include specific MADS box factors (1, 8), pocket proteins (9), Sp1 (10), and runt domain (e.g., Cbfa1) (11–13) transactivators. These cooperative interactions are points of positive and negative regulation in response to growth factors (8, 14–16), cytokines (17, 18), and steroid hormones (19–23). Chromatin remodeling has now emerged as one potential modality for gene activation by Ets proteins (3, 24).

<sup>†</sup> This work was supported by NIH Grants DK52446 and AR43731 to D.A.T. and by the Charles E. Culpeper Foundation. D.A.T. is a Charles E. Culpeper Medical Science Scholar.

<sup>\*</sup> Address correspondence to this author at Merck Research Laboratories, WP26A-1000, West Point, PA 19486. Phone (215) 652-8273; fax (215) 652-4328.

<sup>‡</sup> The first two authors have contributed equivalently to the completion of this work.

<sup>§</sup> Present address: Department of Bone Biology and Osteoporosis Research, Merck & Co., WP26A-1000, West Point, PA 19486.

However, little is known of the molecular mechanisms whereby Ets repressors function to negatively regulate gene expression.

Two homologous interstitial collagenase genes, MMP1<sup>1</sup> (interstitial collagenase, collagenase-1) and MMP13 (collagenase-3), are expressed by vertebrate mesenchymal cells and contribute to the turnover of extracellular matrix during development, connective tissues' responses to injury, and tumor invasion (25). An exception may exist for mice and rats, since these two rodent species apparently lack the endogenous MMP1 gene and express only MMP13 (26, 27). However, in all other mammalian species examined—including guinea pigs (28), rabbits (26), dogs (29), pigs (30), nonhuman primates (31), and humans (32)—MMP1 participates in the physiology and pathophysiology of extracellular matrix remodeling, including bone turnover (33–36). FGF2, a potent autocrine osteoblast growth factor (37, 38), upregulates transcription directed by the rabbit (39) and human (15) MMP1 promoters in osteoblast cellular backgrounds. Analyzing the human MMP1 promoter, we recently mapped this FGF2 transcriptional response to a phylogenetically conserved, bipartite Ets–AP1 element located at nucleotides –100 to –61 relative to the human MMP1 gene transcription initiation site (15). Under basal conditions, the MMP1 promoter is repressed via protein–DNA interactions at the Ets cognate, and supported via protein–DNA interactions at the AP1 cognate (15). In response to FGF2 stimulation of MC3T3E1 calvarial osteoblasts, a minimum of two mechanisms mediate MMP1 promoter upregulation: (a) transcriptional activation via a Fra1/c-Jun-containing complex that binds the AP1 cognate and (b) derepression of promoter activity via unidentified complexes that recognize the Ets cognate. We wished to identify Ets repressors that potentially participate in the regulation of gene expression in the calvarial osteoblast. Therefore, we performed RT-PCR analysis of mRNA isolated from MC3T3E1 cells, using degenerative amplimers to the conserved Ets DNA binding domain and thus surveying the Ets genes expressed by these cells. Six distinct Ets messages were identified: Ets2, Fli1, GABP $\alpha$ , SAP1, Elk1, and PE1. Of these, only PE1 has extensive identity (37%) to a known Ets transcriptional repressor, ERF (40). Since PE1 was initially reported only as a partial cDNA sequence and had never been functionally characterized (41), we cloned murine PE1 cDNA and performed biochemical analysis of this particular Ets family member. The murine PE1 ORF is considerably larger than the previously reported ORF of the human PE1 oncogene. We have isolated a 2 kb cDNA from a mouse brain library

that encodes a predicted 57 kDa, proline-rich protein containing the published N-terminal Ets domain of PE1 and a novel C-terminal domain with extensive interrupted homology to murine ERF. Consistent with the predicted proline-rich open reading frame, affinity-purified rabbit anti-mouse PE1 antibody specifically recognizes a protein migrating with apparent molecular mass of ~66 kDa that is present only in the nuclear fraction of MC3T3E1 murine osteoblasts. Recombinant PE1 protein exhibits DNA binding activity, recognizing functionally important Ets cognates in the MMP1 and osteopontin (OPN) proximal promoters in gel shift assay. Transient transfection studies demonstrate that PE1 is a transcriptional repressor of MMP1 promoter activity and that PE1 suppression maps to the MMP1 promoter region –123 to –61; surprisingly, repression is not dependent upon the MMP1 Ets cognate at –88 to –83, but rather requires the promoter region encompassing the AP1 cognate at –72 to –66. This suggests that PE1 protein–protein interactions downregulate MMP1 promoter activity. Consistent with this notion, addition of recombinant purified GST–PE1 to MC3T3E1 crude nuclear extracts inhibits protein–DNA interactions assembled by the MMP1 AP1 cognate. In toto, these data indicate that PE1 participates in the transcriptional regulation of AP1-dependent MMP1 promoter activity. As observed with other transcriptional repressors of MMP1 gene expression (21, 42, 43), transcriptional suppression by PE1 functions via downregulation of AP1-dependent promoter activity. Since the related Ets suppressor ERF represses prolactin expression by antagonizing Pit1 protein–DNA interactions (44)—again independent of a cis Ets cognate—this mode of negative gene regulation may represent a general mechanism for transcriptional regulation by Ets domain repressors.

## EXPERIMENTAL PROCEDURES

**Chemicals, Cell Culture, Synthetic Oligodeoxynucleotides, and Molecular Biology Reagents.** All chemicals, salts, and buffers for cloning and biochemical analyses were obtained from either Fisher Scientific (St. Louis, MO) or Sigma (St. Louis, MO). All Corning brand cell culture plasticware was purchased from Fisher Scientific. Cell culture medium and serum was obtained from Summit (Fort Collins, CO) or Life Technologies (Gaithersburg, MD). MC3T3E1 mouse calvarial osteoblasts were cultured as described (45) in  $\alpha$ -modified Eagle's medium and 10% fetal calf serum with penicillin/streptomycin. Custom synthetic oligodeoxynucleotides were purchased from Life Technologies (Gaithersburg, MD). Cloning reagents were purchased from Oncor (Gaithersburg, MD), Clontech (Palo Alto, CA), and Amersham Pharmacia Biotech (Piscataway, NJ). Radionuclides were purchased from Amersham (Arlington Heights, IL). Routine molecular biology enzymes and buffers were obtained from Promega (Madison, WI). The high-fidelity, KlenTaq-based Advantage PCR kit was purchased from Clontech (Palo Alto, CA). All clones, subclones, and PCR products were sequenced using the ABI Prism dye terminator kit (Foster City, CA).

**RT-PCR Survey of Ets cDNAs Expressed by Osteoblasts and Cloning of Murine PE1.** A pair of degenerative amplimers DETS1 (5'-TGG CAN TTY YTN YTN SAR TY-3') and DETS2 (5'-RTA RTA RTA NCK NAR NGC NCK-3') were designed to encode conserved regions of the Ets DNA binding domain (annealing position in murine PE1

<sup>1</sup> Abbreviations: BSA, bovine serum albumin; CBP, CREB binding protein; CMV, cytomegalovirus; CSPD, disodium 3-(4-methoxyphosphoryl)-1,2-dioxetane-3,2'-(5'-chloro)-tricyclo[3.3.1<sup>3,7</sup>]decan-4-yl)phenyl phosphate; EDTA, ethylenediaminetetraacetic acid; EGTA, ethylene glycol bis( $\beta$ -aminoethyl ether)-*N,N,N',N'*-tetraacetic acid; FGF2, basic fibroblast growth factor; FGFR, fibroblast growth factor receptor; GST, glutathione S-transferase; HAT, histone acetyltransferase; Hepes, 4-(2-hydroxyethyl)-1-piperazineethanesulfonic acid; Inr, initiator region; IPTG, isopropyl thiogalactoside; LUC, luciferase; MAPK, mitogen-activated protein kinase; MMP, matrix metalloproteinase; MOPS, 3-(*N*-morpholino)propanesulfonic acid; NLS, nuclear localization signal; PBS, phosphate-buffered saline; PCR, polymerase chain reaction; PMSF, phenylmethanesulfonyl fluoride; PVDF, poly(vinylidene difluoride); RAR- $\alpha$ , retinoic acid receptor  $\alpha$ ; RT, reverse transcription; SDS–PAGE, sodium dodecyl sulfate–polyacrylamide gel electrophoresis; kb, kilobase(s); Topo II, topoisomerase II; Tub, tubulin.

```

1 - CGGGAGAGCAGGAGGGCGAAAATGAAAGCAGGCTGTAGCATCGTGGAAAAGCCAGAAGGA
1      M K A G C S I V E K P E G
61 - GGTGGAGGGTATCAGTTTCCGATTGGGCTACAAAGCCGAGTCGTCGCCGGGCTCCCGG
14      G G G Y Q F P D W A Y K A E S S P G S R
121 - CAGATCCAGCTGTGGCACTTCCTGGAAGTCTGTCAGAAGGAAGAGTTCGCCCATGTC
34      Q I Q L W H F I L E L L Q K E E F R H V
181 - ATCGCCTGGCAGCAGGGAGAGTACGGGGAGTTTGTTCATCAAGGATCCAGATGAAGTGGCT
54      I A W Q Q G E Y G E F V I K D P D E V A
241 - CGCCTCTGGGGCCGAGGAAGTGCAACACAGATGAACTATGACAAGCTGAGCCGGGCC
74      R L W G R R K C K P Q M N Y D K L S R A
301 - CTCAGATACTATTACAACAAGAGGATCCTTCATAAAACAAAAGGAAAGGTTTACTAC
94      L R Y Y Y N K R I L H K T K G K R F T Y
361 - AAGTTTAACTTCAACAAGCTCGTGATGCCCAACTACCCGTTTCATCAACATTGCTCGAGT
114      K F N F N K L V M P N Y P F I N I R S S
421 - GGTGTGTTCTCCTCAGAGTGGCCACCAGTGCCAACAGCCTCCTCCCGTTCCATTTCCTCA
134      G V V P Q S A P P V P T A S S R F H F P
481 - CCTCTAGACAGCCATTCTCTACTGGCGATGTGCAACCGGGTCGTTCTCTGCAGCTCA
154      P L D S H S P T G D V Q P G R F S A S S
541 - CTGAGTGCTTCTGGCCCTGAGTCAAGGGTTACCACTGACAGGAAGGTCGAGCCTTCGGAC
174      L S A S G P E S R V T T D R K V E P S D
601 - CTGGAAGATGGCTCGGCCTCTGACTGGCACCAGGGGTCGACTTCATGCCCTCCCGAAAT
194      L E D G S A S D W H R G M D F M P S R N
661 - GCTCTGGGCGGAGGAGCAGTCGGCCACCAGAAACGCAAGCCTGACATACTGCTTCTCTC
214      A L G G G A V G H Q K R K P D I L L P L
721 - TTCACCCGGCCAGCCATGTACCCTGACCCGCGCAGTCCCTTCGCTATCTCTCCGGTCCCT
234      F T R P A M Y P D P R S P F A I S P V P
781 - GGCCGCGGAGGGGTCTTAATGTCCCATCTCACCAGCCCTGTCCCTGACTCCCACCATG
254      G R G G V L N V P I S P A L S L T P T M
841 - TTCTCTACAGTCCCTCACCAGGCCTGAGCCCTTCACCAGCAGCAGTTGCTTCTCCTTC
274      F S Y S P S P G L S P F T S S S C F S F
901 - AACCAGAGGAAATGAAACACTACCTTCATTCTCAAGCCTGTTCCGTTGTTCAACTACCAT
294      N P E E M K H Y L H S Q A C S V F N Y H
961 - CTGAGTCCCCGACTTTCCCCCGTTACCCAGGGCTCATGGTCCCACCGCTGCAGTGCCAA
314      L S P R T F P R Y P G L M V P P L Q C Q
1021 - ATGCATCTGAGGAGCCTTCCAGTTCTCCATCAAGCTGCAGCCCCCGCGGCTGGACGG
334      M H P E E P S Q F S I K L Q P P P A G R
1081 - AAGAACCGCGAGAGGGTAGAGAGCCGGGAGGAGGCTGTTCCGGGCTCTGTGCCCGCCAGC
354      K N R E R V E S R E E A V R G S V P A S
1141 - GCTCCTGTTCCCTCTCGGATTAAGGTAGAGCCGGCCACAGAGAAGGATCCTGACAGCCTC
374      A P V P S R I K V E P A T E K D P D S L
1201 - CGGCAGTCAACCCAGGGAAGGAGGAACAGACCCAAGAAAGTGGACAGCATTTCGGAGCAGG
394      R Q S T Q G K E E Q T Q E V D S I R S R
1261 - ACCATAGAAGAGGGGAAAGGCACCGGGTTTGCCACCCCTCACCACCTGGCCCTCTGTG
414      T I E E G K G T G F A H P S P T W P S V
1321 - TCCATTAGCACTCCCACTGACGAACCCCTAGAGGGGACCGAAGACAGTGAGGACAGGCTC
434      S I S T P S D E P L E G T E D S E D R S
1381 - GCCAGGAGCCCGGTGTACCCGAGAAGAAAGAAGACGCCCTGATGCCCCCTAAGCTTCGG
454      A R E P G V P E K K E D A L M P P K L R
1441 - CTGAAGAGGCGGTGGAATGACGACCTGAAGCCAGGGAGCTCAACAAAACGGGCAAGTTC
474      L K R R W N D D P E A R E L N K T G K F
1501 - CTCTGGAATGGGGCAGGACCCAGGGCTGGCCACAACGGCCACTGCTGCCGCTGATGCT
494      L W N G A G P Q G L A T T A T A A D A
1561 - TAAACCACAGTGGAAGGGAAGCTGTTTCATATTACAATCAAATACACCG - 1610

```

\*

FIGURE 1: cDNA and protein sequence of murine PE1. The sequence of the cDNA encoding murine PE1 protein was obtained from two independent phage clones isolated from a mouse brain cDNA library as described under Experimental Procedures. The upper strand sequence is given, and the contiguous open reading frame encoding murine PE1 is presented (GenBank AF156530). The 513 amino acid open reading frame encodes a Pro-rich basic protein of ~57 kDa, in general agreement with the apparent  $M_r$  observed for MC3T3E1 nuclear PE1 by Western blot (~66 kDa; Figure 3, below). Note that, as observed with ERF (Figure 2A) and Ets1 (GenBank X55757), translation is predicted to initiate from an amino-terminal Met residue immediately followed by a Lys residue. Sequence analysis by ProfileScan confirms that the 82 amino acid Ets domain is encoded by the N-terminal residues 35–116 (boldface type) and that a nuclear localization signal is present at residues 462–479. The PE1 peptide sequence used to generate affinity-purified anti-PE1 rabbit polyclonal antibodies is encoded by residues 351–364. The DNA sequence corresponding to the annealing positions of the degenerate sense and antisense amplimers in the conserved Ets domain is underlined. See text for additional details.

indicated by underlined DNA sequence in Figure 1). These primers were used in RT-PCR reactions with RNA extracted from MC3T3E1 murine calvarial osteoblasts by techniques previously described (45). RT-dependent PCR fragments of appropriate size (0.2 kb) were gel-purified, 5'-phosphorylated,

blunt-ligated into pUC19, and sequenced by the ABI Prism dye terminator method (Foster City, CA), and sequences were compared with combined databases by use of the NCBI BLAST search. Of 20 cloned inserts initially sequenced, three encoded Ets2, three contained Fli1, three encoded PE1, one



contained SAPI1, one contained Elk1, one contained GABP $\alpha$ , and eight contained non-Ets inserts. Since the PE1 sequence was the only Ets domain cDNA identified that had homology to a known Ras-regulated Ets repressor, human ERF, we cloned murine PE1 to characterize this protein biochemically. A commercially available, random hexamer-primed mouse brain  $\lambda$ gt11 cDNA library (Clontech catalogue ML3000b, Palo Alto, CA) was screened with radiolabeled random hexamer-primed probes derived from the rat PE1 Ets domain (kind gift of Dr. R. Hromas) by techniques previously described (46). Subcloning was performed by high-fidelity PCR (vide infra), with amplimers that anneal upstream (5'-GAC TCC TGG AGC CCG TCA G-3') and downstream (5'-GAC ACC AGA CCA ACT GGT AAT G-3') of the  $\lambda$ gt11 polylinker. Briefly, phage plugs were eluted overnight at 4 °C in 1 mL of 35 mM Tris-HCl, pH 7.5/100 mM NaCl/10 mM MgSO<sub>4</sub> with 20  $\mu$ L of chloroform. Phage DNA was ejected from 5  $\mu$ L of phage eluate by denaturing for 5 min at 95 °C. Insert DNA was amplified by the Advantage PCR system (Clontech, Palo Alto, CA), with cycling parameters of 94 °C  $\times$  15 s, 55 °C  $\times$  30 s, and 72 °C  $\times$  4 min for 30 cycles after a 94 °C  $\times$  1 min preamplification treatment to activate the KlenTaq polymerase. After amplified inserts were tailed for 7 min at 72 °C, inserts were subcloned into the pGEM-T Easy Vector (Promega, Madison, WI) and sequenced with the ABI Prism dye terminator kit (Foster City, CA). Sequence analysis was performed with ProfileScan software accessible from the ISREC Bioinformatics home page (Swiss Institute for Experimental Cancer Research; the URL is <http://www.isrec.isb-sib.ch/index.html>), and DNA-MAN version 4.0 software for Windows 95 purchased from Lynnon BioSoft (Vandrevil, Quebec, Canada).

**Generation of Affinity-Purified Polyclonal Antibodies and Western Blot Analyses.** A small, Cys-initiated synthetic peptide corresponding to the murine PE1 protein residues 351–364 (AGRKNRERVESREE; see Figure 1, GenBank AF156530) were coupled to keyhole limpet hemocyanin, and rabbit anti-peptide polyclonal sera generated by Zymed Laboratories, Inc. (South San Francisco, CA). Purified GST and GST–PE1 recombinant proteins were prepared by techniques previously detailed and covalently coupled to cyanogen bromide-activated Sepharose (47). All preimmune and immune sera were presorbed with GST–Sepharose. Subsequently, 5 mL of rabbit anti-PE1 peptide immune serum (diluted with 45 mL of 10 mM Tris-HCl, pH 7.5) was adsorbed to 0.2 mL of GST–PE1–Sepharose and washed with 25 volumes each of 10 mM Tris-HCl, pH 7.5 and 10 mM Tris-HCl, pH 7.5/500 mM NaCl. Anti-PE1 antibody was sequentially eluted with 4  $\times$  0.5 mL of 100 mM glycine, pH 2.5, and each eluate neutralized with 50  $\mu$ L of 1 M Tris, pH 8. Purified anti-PE1 fractions were first assessed in Western blot analyses with 1  $\mu$ g of aliquots of recombinant purified PE1 protein expressed in *Escherichia coli*. Typically, 1:500 to 1:2000 dilution of affinity-purified anti-PE1 polyclonal antibodies were used in all Western blot analyses. Immune complexes were visualized by chemiluminescent detection with alkaline phosphatase-conjugated goat anti-rabbit antibody (1:5000 dilution) and CSPD (Tropix, Bedford, MA) as previously described (48).

**Biochemical Fractionation of MC3T3E1 Cell Extracts.** MC3T3E1 cells were plated on 15 cm diameter tissue culture dishes (10<sup>5</sup> cells/cm<sup>2</sup>), and cultured for an additional 3 days

with fresh medium changes every other day. After cell cultures were rinsed twice with ice-cold PBS, cells were scraped into PBS and collected by centrifugation at 1600 rpm  $\times$  5 min. Subsequently, cells were extracted and fractionated into cytosolic (Cyto) and crude nuclear (Nuc) fractions following the protocol of Dignam et al. (49). Protein recovery in each fraction was determined by the bicinchoninic acid assay (Pierce, Rockford, IL) after removing contaminants following the method of Peterson (50). Twenty-microgram aliquots of cytosolic and nuclear protein fractions were resolved by SDS–PAGE (12% acrylamide gels; Novex, San Diego, CA) and electrotransferred to a PVDF membrane. Western blot analysis was used to characterize PE1 protein enrichment in nuclear vs cytosolic fractions, monitoring tubulin (cytosolic marker) (51) and topoisomerase II (nuclear marker) (52) immunoreactivity in these aliquots to verify the fidelity of the biochemical fractionation. Prestained protein standards (rainbow markers, Amersham, Rockford, IL) were used to estimate relative molecular mass of immunoreactive proteins after electrotransfer and immunovisualization. Recombinant purified GST–PE1 was used as a positive control for the immunoreactivity of the anti-PE1 antibody; GST was used as a negative control. Anti-topoisomerase II antibody was purchased from TopoGen (catalogue no. 2011-1, Columbus, OH). Anti-tubulin antibody TU-01 was purchased from Zymed (South San Francisco, CA). Typically, these antibodies were used at 1:500–1:2000 dilutions in Western blot analyses (vide supra).

**Assessment of GST–PE1 DNA Binding Activity by Electrophoretic Mobility Gel Shift Assays.** Recombinant GST–PE1 was expressed in *E. coli* from the prokaryotic expression vector pGEX-2T (Amersham–Pharmacia, Piscataway, NJ) as described previously (48), purified by glutathione–agarose affinity chromatography, and dialyzed exhaustively against the crude nuclear extraction buffer D of Dignam et al. (49). Synthetic oligodeoxynucleotides corresponding to the designated promoter regions of the human MMP1 and murine OPN promoters were 5'-radiolabeled with [ $\gamma$ -<sup>32</sup>P]ATP and T4 polynucleotide kinase as previously described (53). Aliquots (~50 ng) of recombinant GST or GST–PE1 were assayed for formation of protein–DNA complexes by gel shift assay and autoradiography. Gel shift assays were carried out as previously detailed (53) in the presence of excess (10  $\mu$ g) BSA. Typically, 0.1 pmol of radiolabeled probe was present in the standard 20  $\mu$ L binding reaction. Cold competition assays with duplex DNA (dsDNA) were formed with annealed synthetic duplex oligodeoxynucleotides corresponding to sequences in Figure 5B. The GenBank accession number for the human MMP1 promoter is M16567; the GenBank accession number for the murine OPN promoter is M38399.

**Cellular Transient Transfection Assays.** The construction of the human MMP1 promoter–luciferase reporter 5'-deletion constructs 179 MMPLUC (–179 to +63), 75 MMPLUC (–75 to +63), and 50 MMPLUC (–50 to +63) has already been detailed (15). The heterologous promoter construct MMP1 (–123 to –61) RSVLUC (15) and the RSVLUC minimal promoter–reporter (54) were constructed as previously detailed. The murine OPN–promoter–luciferase reporter constructs 636 OPNLUC (–636 to +58), 107 OPNLUC (–107 to +58), and 61 OPNLUC (–61 to +58) were obtained by applying PCR (mouse genomic DNA

<b>A.</b>	MOUSE PE1	<u>MKAGCSIVEKPEGGGGYQFPDWAYKAESSPGSRQIQLWHFILELLQKEEFRHVIAWQQGEYGEFVIKDPD</u>	70
	MOUSE ERF	<u>MK.....TPADTGFATFPDWAYKESSPGSRQIQLWHFILELLRKEEYQGVIAW.QGDIYGEFVIKDPD</u>	61
	HUMAN ERF	<u>MK.....TPADTGFATFPDWAYKESSPGSRQIQLWHFILELLRKEEYQGVIAW.QGDIYGEFVIKDPD</u>	61
	MOUSE PE1	<u>EVARLWGRRKCKPQMNYDKLSRALRYYYNKRILHKTGKRFTYKFNENKLVMPNYPFINIRSSGV.VPQS</u>	139
	MOUSE ERF	<u>EVARLWGRRKCKPQMNYDKLSRALRYYYNKRILHKTGKRFTYKFNENKLVMPNYPFINIRSSGV.VPQS</u>	131
	HUMAN ERF	<u>EVARLWGRRKCKPQMNYDKLSRALRYYYNKRILHKTGKRFTYKFNENKLVMPNYPFINIRSSGV.VPQS</u>	131
	MOUSE PE1	<u>APPVPTASSRFHFPPLDSH...SPTIGDVQPGFRFSASSLSASGPESRVTTDRKVEPSDLEDGSASDWHRGM</u>	206
	MOUSE ERF	<u>APPVPSGGSHFRFPSTPSEVLSPTEIPRSPACSSSSSLFSAVVARRLRGGSVSDCSGTSELEEPLG</u>	201
	HUMAN ERF	<u>APPVPSGGSHFRFPSTPSEVLSPTEIPRSPACSSSSSLFSAVVARRLRGGSVSDCSGTSELEEPLG</u>	201
	MOUSE PE1	<u>DFMPSRNALGGGAVGHQKRKPDILLPLFTRPAMYDPFR.....SPFAISPVPGRGVINVPISPALSIT</u>	270
	MOUSE ERF	<u>EDPRARPPGPPELGAFRGPPLARLPHDPGVFRVYHPRGGPELSPFPVSHLAGGSLIPPOLSPALPMT</u>	271
	HUMAN ERF	<u>EDPRARPPGPPELGAFRGPPLARLPHDPGVFRVYHPRGGPELSPFPVSHLAGGSLIPPOLSPALPMT</u>	271
	MOUSE PE1	<u>PTMFSYSPSPGLSHFTSSC.....FSFNPEEMKHYLHSAQSVFNHYLSPTTFPRYPGLM...</u>	326
	MOUSE ERF	<u>PTHLAYTPSPITLSMYPSGGGGPSGGGGSHFSFSPEDMKRYLQAHTQSVNYHLSPTTFPRYPGLVVPQ</u>	341
	HUMAN ERF	<u>PTHLAYTPSPITLSMYPSGGGGPSGGGGSHFSFSPEDMKRYLQAHTQSVNYHLSPTTFPRYPGLVVPQ</u>	341
	MOUSE PE1	<u>.....VHPLOQMHPPEPSQFSIKLOPPFAGRKNRERVESREEAVRGSVPASAPVPS</u>	378
	MOUSE ERF	<u>PQRDPKCPLPMPAPETPFVSSASSSSSSSSSFFKFKLOPPHGRQHAAGEKAPGGTDKSSGGSGSGL</u>	411
	HUMAN ERF	<u>PQRDPKCPLPMPAPETPFVSSASSSSSSSSSFFKFKLOPPHGRQHAAGEKAVAAADK.SGSSA.GGL</u>	409
	MOUSE PE1	<u>RIKVEPATEKDPDSLRSQSTQGKEEQTOEVDIRSRTIEEGKGTGFAHPSPTWPSVSISTPSDEPLEGTED</u>	448
	MOUSE ERF	<u>AEGAGAVAPPPPPQIKVEPISEGESEEVETDISD.....ED</u>	449
	HUMAN ERF	<u>AEGAGALAPPPPPQIKVEPISEGESEEVETDISD.....ED</u>	447
	MOUSE PE1	<u>SEDRSARE.....PGVPEKKEDALMPPKRLKRRWNDPEARELNKTGKFLWNGAGPQG</u>	502
	MOUSE ERF	<u>EEDGEVFKTPRAPPPAPKPEPGEAPGVAQC....MELKLEKRRWSEDCRLEGGGCLSGGPEDEGEDKK</u>	514
	HUMAN ERF	<u>EEDGEVFKTPRAPPPAPKPEPGEAPGASQC....MELKLEKRRWSEDCRLEGGGCPAGGFEDEGEDKK</u>	512
	MOUSE PE1	<u>LATT.....ATAAADA</u>	513
	MOUSE ERF	<u>VRGDVGPGESGGPLTPRRVSSDLOHATAQLSLEHRDS</u>	551
	HUMAN ERF	<u>VRGE.GPGEAGGPLTPRRVSSDLOHATAQLSLEHRDS</u>	548

<b>B.</b>	MOUSE PE1	<u>MKAGCSIVEKPEGGGGYQFPDWAYKAESSPGSRQIQLWHFILELLQKEEFRHVIAWQQGEYGEFVIKDPD</u>	70
	Hu PE1 CORR	<u>MKAGCSIVEKPEGGGGYQFPDWAYKAESSPGSRQIQLWHFILELLQKEEFRHVIAWQQGEYGEFVIKDPD</u>	70
	Hu PE1 FSM	<u>MKAGCSIVEKPEGGGGYQFPDWAYKAESSPGSRQIQLWHFILELLQKEEFRHVIAWQQGEYGEFVIKDPD</u>	70
	MOUSE PE1	<u>EVARLWGRRKCKPQMNYDKLSRALRYYYNKRILHKTGKRFTYKFNENKLVMPNYPFINIRSSGVVPQSA</u>	140
	Hu PE1 CORR	<u>EVARLWGRRKCKPQMNYDKLSRALRYYYNKRILHKTGKRFTYKFNENKLVMPNYPFINIRSSGVVPQSA</u>	140
	Hu PE1 FSM	<u>EVARLWGRRKCKPQMNYDKLSRALRYYYNKRILHKTGKRFTYKFNENKLVMPNYPFINIRSSGVVPQSA</u>	140
	MOUSE PE1	<u>PPVPTASSRFHFPPLDSHSPITIGDVQPGFRFSASSLSASGPESRVTTDRKVEPSDLEDGSASDWHRGMDFMP</u>	210
	Hu PE1 CORR	<u>PPVPTASSRFHFPPLDTHSPITIGDVQPGFRFSASSLSASGPESRVTTDRKVEPSDLEDGSASDWHRGMDFMP</u>	210
	Hu PE1 FSM	<u>PPVPTASSRFHFPPLDTHSPITIGDVQPGFRFSASSLSASGPESRVTTDRKVEPSDLEDGSASDWHRGMDFMP</u>	210
	MOUSE PE1	<u>SRNALGGGAVGHQKRKPDILLPLFTRPAMYDPFRSPFAISPVPGRGVINVPISPALSITPTMFSYSPSP</u>	280
	Hu PE1 CORR	<u>SRNAIGGGGIGHQKRKPDIMLPLFARPGMYDPHSPFAVSPIPGRGGVINVPI</u>	262
	Hu PE1 FSM	<u>PGMPLVEEGLAIRNASLT</u>	228
	MOUSE PE1	<u>GLSPFTSSSCFSFNPEEMKHYLHSAQSVFNHYLSPTTFPRYPGLMVPPLOQMHPPEPSQFSIKLOPPP</u>	350
	Hu PE1 CORR		
	Hu PE1 FSM		
	MOUSE PE1	<u>AGRKNRERVESREEAVRGSVPASAPVPSRIKVEPATEKDPDSLRSQSTQGKEEQTOEVDIRSRTIEEGKG</u>	420
	Hu PE1 CORR		
	Hu PE1 FSM		
	MOUSE PE1	<u>TGFAHPSPTWPSVSISTPSDEPLEGTEDSEDRSAREPGVPEKKEDALMPPKRLKRRWNDPEARELNKT</u>	490
	Hu PE1 CORR		
	Hu PE1 FSM		
	MOUSE PE1	<u>GKFLWNGAGPQGLATTATAAADA</u>	513
	Hu PE1 CORR		
	Hu PE1 FSM		

FIGURE 2: Protein sequence comparison of PE1 and ERF. (A) The protein sequence predicted from the murine PE1 cDNA (GenBank accession no. AF156530) was compared to that predicted for the murine ERF (U58533), and human ERF (U15655). Note that murine PE1 has 37% identity with murine and human ERF. Further note that in addition to the Ets domain, significant identity also exists between murine PE1 and ERF in N- and C-terminal regions. (B) Comparison of murine and human PE1 protein sequences. Hu PE1 FSM, human PE1 protein sequence predicted from the reported cDNA sequence (GenBank L16464) that likely has a frameshift mutation introduced by a nucleic acid deletion. Hu PE1 CORR predicted human PE1 protein sequence after correction by introducing the missing nucleic acid from the murine cDNA sequence. Note that the human PE1 protein predicted from the reported human PE1 ORF would produce a truncated protein that lacks the nuclear localization signal present in murine PE1 residues 462–479 (Figure 1). After correction for this probable frameshift in the human PE1 cDNA, the extended identity between the partial human PE1 protein sequence and the complete murine PE1 protein sequence becomes evident.

as initial template) to amplify the indicated OPN promoter segments with 5'-*KpnI* and 3'-*MluI* linkers by techniques previously described (53). The OPN promoter fragments were directionally subcloned in to the *KpnI* and *MluI* sites of pGL2Basic (Promega, Madison, WI) and sequenced. The CMV-PE1 eukaryotic expression construct was generated by introducing 5'-*KpnI* and 3'-*BglIII* (with stop codon) restriction sites onto the cDNA fragment encoding full-length PE1 residues 1–513, subcloned into the *KpnI/BamHI* sites of pcDNA3 (Invitrogen, Carlsbad, CA) downstream of the CMV promoter and FLAG epitope tag (48) in good Kozak context (55). MC3T3E1 calvarial osteoblasts were plated in Costar 6 well cluster dishes (35 mm diameter wells,  $7 \times 10^5$  cells/well). Cells were transiently transfected the following day by calcium phosphate-precipitated DNA and osmotic shock as previously detailed (48). All transfections incorporate a promoter-LUC reporter construct (to monitor MMP1 promoter-dependent transcription), a CMV- $\beta$ -galactosidase construct (to control for transfection efficiency), and varying amounts of pcDNA3-PE1 expression construct as indicated. Empty pcDNA3 expression plasmid was added to maintain a constant amount of DNA in each precipitation and transfection. Two days following transfection, cultures were refed with fresh medium containing either vehicle or 3 nM FGF2 and analyzed the following day for luciferase and  $\beta$ -galactosidase activities as previously detailed (48). All results presented were observed in a minimum of two independent replicate experiments.

## RESULTS

*Mouse PE1, an Ets Gene Expressed in MC3T3E1 Osteoblasts, Has Extensive Homology to the Ets Repressor ERF.* We had previously demonstrated that DNA-protein interactions at an Ets cognate in the proximal human interstitial collagenase/MMP1 promoter participate in (i) basal promoter suppression and (ii) FGF2-dependent promoter activation in MC3T3E1 calvarial osteoblasts (15). To identify Ets repressors that potentially participate in this response, we performed RT-PCR analysis of mRNA isolated from MC3T3E1 osteoblasts, using degenerative amplimers to the conserved Ets DNA binding domain to survey the Ets genes expressed by these cells. Six distinct Ets mRNAs were identified: Ets2, Fli1, GABP $\alpha$ , SAP1, Elk1, and PE1. Of the six Ets proteins encoded by these mRNAs, only PE1 has significant homology to a known Ets repressor, ERF (40). However, PE1 has not been characterized biochemically, reported only as partial cDNA sequence and a message expressed by certain leukemia cell lines (41). Therefore, we used a PCR fragment obtained from the rat PE1 Ets domain as a template (kind gift of Dr. R. Hromas) to clone a 2 kb mouse PE1 cDNA from a commercially available brain cDNA library. As shown in Figure 1, the predicted ORF for mouse PE1 encodes a

513 amino acid basic protein ( $pI = 9.07$ ), rich in Pro (11.5% mol/mol) and Ser (10.5% mol/mol). As observed with human and murine ERF and human and murine Ets1, translation initiates with an amino-terminal Met residue immediately followed by a Lys residue. Sequence analysis (ProfileScan) confirms the Ets domain sequence in murine PE1 residues 35–116 and a nuclear localization signal at residues 462–479 (Figure 1). The murine PE1 protein has 37% sequence identity with murine ERF, 37% identity with human ERF, 33% identity with the reported human PE1 ORF, and 6.7% identity with murine Ets1. In contrast to the prototypic Ets activator Ets1, both PE1 and ERF have their Ets domains localized to the N-terminal region of the molecule (Figures 1 and 2A). Like the human PE1 Ets domain (Figure 2B), the murine PE1 Ets domain is 82 amino acids in length, one amino acid longer than the ERF Ets domain due to an additional Gln residue in the Ets domain sequence (Figure 2A, residue 57 in the PE1 protein sequence). Significant (~37%) identity exists between murine PE1 and murine ERF or human ERF beyond the Ets DNA binding domain. Closest identity is noted in sequences immediately N- and C-terminal to the Ets domain, but also extends in short motifs throughout the C-terminal domain of murine PE1 (Figure 2A). The MAPK-regulated Thr phosphorylation consensus Pro-Leu-Thr-Pro (40) present in ERF (Thr-526 human ERF, Thr-529 in murine ERF) is lacking in murine PE1 (Figure 2). Of note, the reported partial/incomplete ORF for the human PE1 cDNA (i) diverges from the murine PE1 sequence at PE1 residue 173 and truncates 55 residues downstream from this point, (ii) would lack the C-terminal homology with the related Ets protein ERF, and (iii) would lack the nuclear localization signal at residues 462–479. On the basis of cDNA sequence comparison between murine PE1 and human PE1, the reported human PE1 cDNA sequence most probably contains a frameshift mutation that results in a truncated ORF. After correction for this frameshift, the extended identity between the incomplete human PE1 protein sequence (41) and the complete murine PE1 protein sequence is evident (Figure 2B).

*Murine Osteoblast PE1 Is a Nuclear Protein of  $M_r = 66$  kDa.* We wished to characterize the size and localization of the endogenous PE1 protein expressed by MC3T3E1 murine osteoblasts. Therefore, cytosolic and nuclear fractions were prepared by the method of Dignam et al. (49) and extracted proteins were analyzed by Western blot analyses with affinity-purified rabbit anti-PE1 polyclonal antibodies generated as described under Experimental Procedures. As shown in Figure 3A, a protein that migrates with an apparent molecular mass of 66 kDa was immunovisualized with anti-PE1 antibody that localizes exclusively in the nuclear fraction of MC3T3E1 cells. The apparent molecular mass and nuclear localization of the endogenous PE1 protein is in good



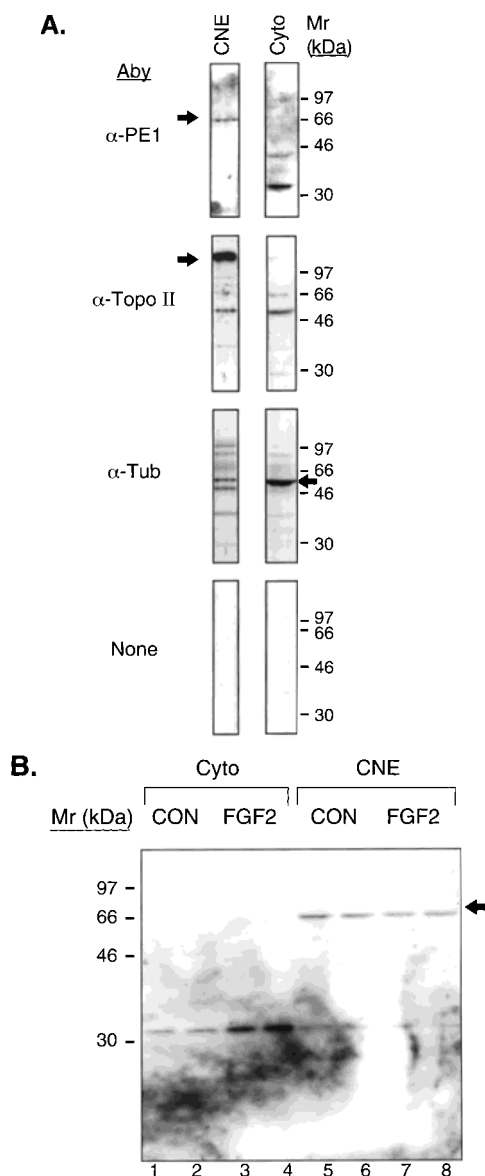


**FIGURE 3:** Western blot analysis of endogenous murine PE1 protein accumulation. Cell extracts prepared from MC3T3E1 osteoblasts were biochemically fractionated into crude nuclear (CNE) and cytoplasmic (Cyto) fractions following the method of Dignam et al. (49). (A) PE1 protein was immunovisualized by Western blot analysis of CNE and Cyto fractions as described under Experimental Procedures. The efficiency of cellular fractionation was verified by monitoring topoisomerase II (Topo II) and tubulin (Tub) immunoreactivity as markers of CNE and Cyto fractions, respectively. Arrows indicate the respective immunoreactive bands that represent to the corresponding full-length PE1, Topo II, and Tub proteins. In general agreement with the predicted PE1 protein product and NLS (Figure 1), a 66 kDa protein immunoreactive with affinity-purified anti-PE1 antibody is identified solely in the nuclear fraction of MC3T3E1 cells, cosegregating with Topo II but not Tub. Smaller anti-PE1 immunoreactive proteins of 35 and 46 kDa are also observed but only in the cytoplasmic fraction and may represent proteolytic fragments. (B) PE1 was immunovisualized in Cyto and CNE fractions of MC3T3E1 cells treated for 24 h with either vehicle control (Con) or 3 nM FGF2. Each adjacent pair of lanes (1 and 2; 3 and 4; 5 and 6; 7 and 8) shows results obtained from independent duplicate treatments. Lanes 5 and 6 are nuclear fractions corresponding to cytosolic fractions 1 and 2, respectively. Lanes 7 and 8 are nuclear fractions corresponding to cytosolic fractions 3 and 4, respectively. Note that FGF2 treatment does not regulate the accumulation of full-length nuclear PE1 protein (arrow) but slightly increases the accumulation of the smaller 35 kDa immunoreactive protein in the cytoplasmic fraction. See text for details.

agreement with the protein predicted by our cDNA (Figures 1 and 2), particularly given the proline-rich sequence of the PE1 protein (i.e., decreases SDS binding and slightly decreases charge density and thus protein mobility on SDS-PAGE). The efficiency of biochemical fractionation was confirmed by use of antibodies for Tubulin (Tub) and topoisomerase II (Topo II), proteins that demarcate cytosolic (51) and nuclear fractions (52), respectively (Figure 3A). A smaller protein of molecular mass 35 kDa was also identified, recognized by anti-PE1 antibody, that accumulates primarily in the cytosolic fraction. While FGF2 treatment has no effect on steady-state levels of the nuclear, full-length 66 kDa PE1 protein (Figure 3B, lanes 5–8), FGF2 does promote accumulation of the immunoreactive 35 kDa protein in the cytoplasm. Thus, consistent with its cDNA sequence, proline-rich character, Ets DNA binding domain, and nuclear localization signal, endogenous full-length PE1 is a nuclear protein that migrates with an apparent molecular mass of 66 kDa. FGF2 does not regulate nuclear PE1 protein accumulation.

*Recombinant Purified GST-PE1 Recognizes Authentic Ets DNA Binding Cognates.* Although the presence of an Ets domain in PE1 strongly implies DNA binding activity, we wished to directly verify this notion. Ets domain proteins classically recognize degenerate cognates of the sequence MGGAWG (M = A or C; W = A or T); the best-characterized high-affinity cognates contain AGGAAG as a core sequence (1). In osteoblasts, the MMP1 (15) and OPN (13) promoters have been identified as possessing Ets DNA binding cognates that are important for promoter activity. Therefore, recombinant purified murine PE1 was prepared as described under Experimental Procedures and then tested for DNA binding activity in gel shift assay with radiolabeled duplex oligonucleotides corresponding to the authentic Ets domain binding cognates of the OPN (13) and MMP1 (15) promoters as probes. As shown in Figure 4, recombinant purified GST-PE1 avidly binds the authentic AGGAAG Ets cognate of the OPN promoter (Figure 4, lanes 4–6); by contrast, GST does not bind Ets cognates at all (Figure 4, lanes 1–3), confirming the role of mPE1 in the observed DNA binding activity. Similar results are obtained with the radiolabeled MMP1 Ets cognate (AGGATG), although binding is ca. 10% that observed with the OPN Ets cognate (data not shown). Competition studies reveal that, as seen with other Ets-domain proteins, an intact GGAAG cognate core is required for mPE1 protein–DNA interactions (Figure 5). While the unlabeled homologous duplex oligonucleotide is able to compete for binding (Figure 5A, lanes 1–3), mutant oligonucleotides containing G to T substitutions in this core sequence cannot compete efficiently (Figure 5A, lanes 4–6, 13–15, 16–19; see also Figure 5B). Similar G to T substitutions outside of the cognate core do not affect binding in competition assays; such mutants—Mut 2 and Mut 3 (Figure 5B)—are as active as the wild-type Ets oligo as competitors for PE1 binding to the radiolabeled Ets cognate (compare Figure 5A lanes 7–9 and 10–12 with lanes 1–3). Thus, PE1 is an authentic DNA binding protein that recognizes the authentic GGAWG core motif of the Ets cognate.

*Transient Expression of PE1 Suppresses the MMP1 Promoter.* As mentioned above, the homology of mPE1 to the related Ets protein ERF strongly suggests that PE1 may

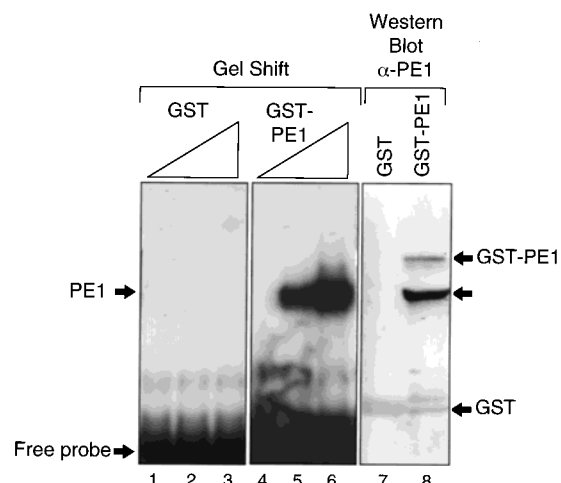
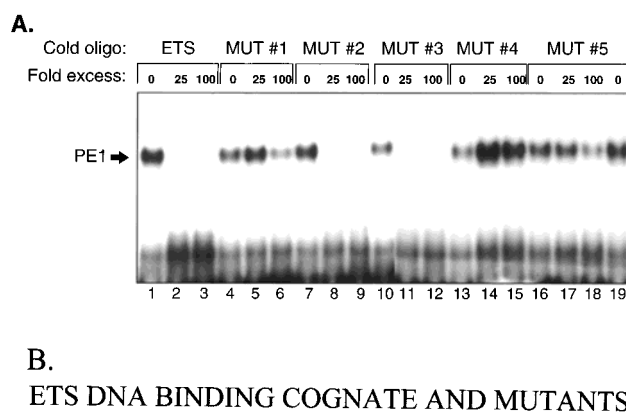


FIGURE 4: Recombinant purified PE1 binds at Ets cognate in gel shift assays. Recombinant GST-PE1 and GST were expressed in *E. coli* and purified as described under Experimental Procedures. Lanes 1–6, gel shift assay; lanes 7 and 8, Western blot analysis with anti-PE1 antibody. Electrophoretic gel mobility shift assays were subsequently carried out using radiolabeled duplex oligonucleotides corresponding to an authentic AGGAAG Ets cognate. Note that while recombinant purified GST does not bind the Ets probe (lanes 1–3), recombinant GST-PE1 avidly binds this duplex Ets cognate (lanes 4–6). Western blot analyses of recombinant purified GST and GST-PE1 with anti-PE1 antibody confirm the presence of the PE1 epitope in GST-PE1 (lane 8) but not in GST (lane 7). The upper pair of arrows indicate the positions of full-length recombinant purified GST-PE1 and a partially degraded product on SDS-PAGE; the lower arrow indicates the position of purified GST. See text for details.

in fact be a transcriptional repressor. To directly test this notion, we transiently expressed PE1 from the CMV promoter (pcDNA3-PE1) in MC3T3E1 osteoblasts, examining effects on the 0.2 kb human MMP1 promoter (luciferase reporter), a promoter active in osteoblasts that contains an Ets cognate at –88 to –83 important for transcriptional activity (15). As shown in Figure 6A, transient expression of PE1 suppresses both basal and FGF2-stimulated promoter activity driven by MMP1 promoter fragment –179 to +63 (179 MMPLUC). In a similar fashion, PE1 expression also downregulated the Ets-dependent mouse OPN promoter (not shown). As previously described (15), 5'-deletions that remove the Ets cognate at –88 to –83 decrease activation by FGF2, since 75 MMPLUC is not inducible. Surprisingly, however, PE1 is still capable of suppressing basal promoter activity driven by MMP1 promoter fragment –75 to +63, in either the presence or absence of FGF2 (Figure 6A, see 75 MMPLUC); PE1 suppression is observed even though this MMP1 promoter fragment lacks the Ets cognate at –88 to –82. Further 5'-deletion of nucleotides –75 to –51 removes the AP1 cognate at –72 to –66 and decreases basal activity in osteoblasts. Coexpression of PE1 has little effect on basal promoter activity driven by the MMP1 promoter fragment –50 to +63 (Figure 6A, 50 MMPLUC). Overexpression of the Ets repressor does weakly decrease the minimal promoter activity driven by the TATA box and Inr, suggesting potential interactions with a component of the preinitiation complex (56) (see Discussion). However, heterologous promoter experiments confirm that the PE1-suppressive response is largely dependent upon MMP1 promoter region encompassing the AP1 cognate encoded by nucleotides –75 to –51 (15); as shown in Figure 6B, the



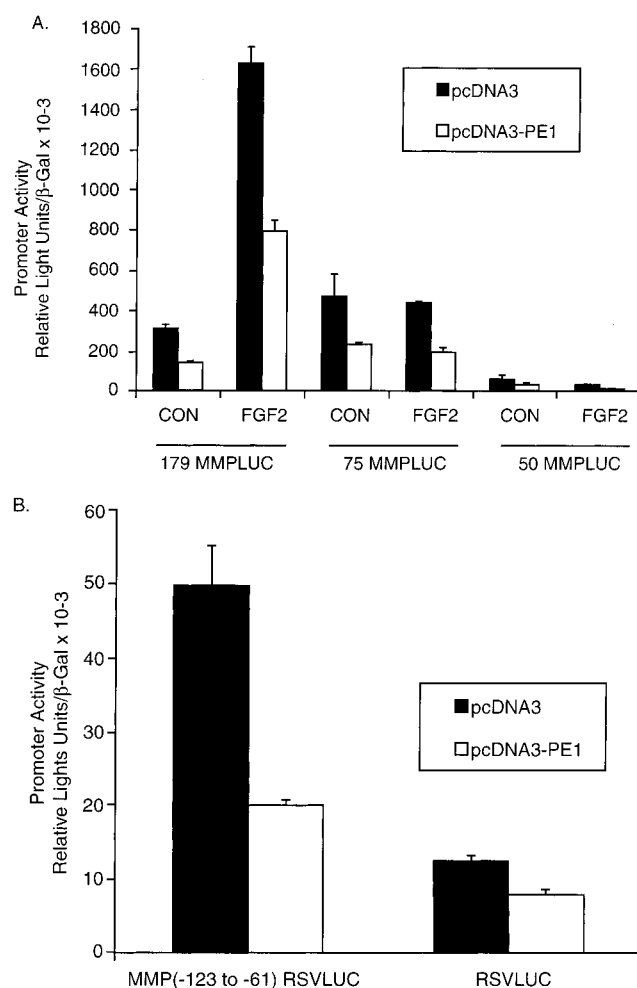
ETS	CAG AGG <u>AGG AAG</u> TGT AGG
MUT #1	CAT ATT <u>ATT AAT</u> TGT AGG
MUT #2	CAT AGG <u>AGG AAG</u> TGT AGG
MUT #3	CAT ATT <u>AGG AAG</u> TGT AGG
MUT #4	CAT AGG <u>ATT AAG</u> TGT AGG
MUT #5	CAT AGG <u>AGG AAT</u> TGT AGG

FIGURE 5: Recombinant purified PE1 recognizes the GGAAG core of authentic Ets domain DNA binding cognates. Recombinant purified GST-PE1 was assessed for DNA binding activity by use of a radiolabeled Ets DNA binding cognate. (A) Binding specificity was determined by competition with either the unlabeled homologous duplex oligo (lanes 1–3) or one of five different mutant duplex oligos (lanes 4–19) in the gel shift assay. Note that the unlabeled homologous oligo with the intact Ets AGGAAG cognate efficiently competes for binding. Further note that Mut 1 (lanes 4–6), Mut 4 (lanes 13–15), and Mut 5 (lanes 16–19) duplex oligos do not compete; all three of these mutants contain T for G transversions that disrupt the AGGAAG cognate (panel B). Finally, note that Mut 2 (lanes 7–9) and Mut 3 (lanes 10–12) were as effective as the wild-type oligo (lane 1–3) in competition; these latter mutant duplex oligos possess T for G transversions that do not disrupt the MGGAWG core necessary for Ets factor recognition. (B) Upper-strand sequences of the duplex synthetic oligodeoxynucleotides used for these studies. This authentic Ets DNA cognate is derived from the proximal mouse OPN promoter (13). Similar results are observed in gel shift assay using the AGGATG Ets cognate from the MMP1 promoter (not shown). See text for details.

transcriptional activity of MMP(–123 to –61)RSVLUC is robustly suppressed by transient PE1 expression. By contrast, PE1 has little effect on transcription driven by the basal RSV promoter (Figure 6B, RSVLUC). Additionally, the basal osteocalcin promoter (53) is not suppressed by PE1 expression in transient transfection assays (not shown). Thus, transcriptional suppression of the MMP1 promoter by PE1 does not require the intact Ets cognate at –88 to –83; rather, by 5'-deletion analysis and heterologous promoter experiments, PE1 suppression maps to the 15 base-pair region –75 to –61, encompassing the AP1 DNA binding cognate at –72 to –66.

**PE1 Inhibits AP1 Protein–DNA Interactions That Support MMP1 Promoter Activity in MC3T3E1 Osteoblasts.** The observation that PE1 can suppress MMP1 transcription independent of the cis-Ets DNA binding cognates suggests that PE1 may be functioning by usurping other protein–DNA interactions that support promoter activity. As mentioned above, for the MMP1 gene, multiple labs—including our own—have demonstrated that protein–DNA interactions





**FIGURE 6:** PE1 suppression of the MMP1 promoter maps to nucleotides  $-75$  to  $-61$  encompassing the AP1 DNA binding cognate at  $-72$  to  $-66$ . (A) MC3T3E1 calvarial osteoblast cell cultures were transfected with 179 MMPLUC, 75 MMPLUC, and 50 MMPLUC promoter-luciferase reporter constructs ( $2 \mu\text{g}/\text{well}$ ) as detailed under Experimental Procedures, along with either pcDNA3 or pcDNA3-PE1 expression plasmid ( $1.5 \mu\text{g}/\text{well}$ ) as indicated. CMB- $\beta$ -galactosidase ( $700 \text{ ng}/\text{well}$ ) was included as an internal control for transfection efficiency, and empty pcDNA3 expression vector was used to maintain constant DNA concentrations in all transfections. Two days following transfection, cell cultures were treated either with vehicle or with  $3 \text{ nM}$  FGF2 to  $20 \text{ h}$ . Subsequently, extracts were prepared for assays of luciferase and  $\beta$ -galactosidase activity. Data are presented as the mean ( $\pm$ SD) luciferase activity observed in independent triplicate transfections. Note that pcDNA3-PE1 suppresses both the basal and FGF2-stimulated promoter activity of 179 MMPLUC. As previously demonstrated (15), FGF2 does not stimulate the proximal MMP1 promoter lacking the Ets DNA binding cognate at  $-88$  to  $-83$  (compare FGF2 induction of 179 MMPLUC with 75 MMPLUC in the absence of PE1); however, PE1 expression still suppresses basal 75 MMPLUC activity in the presence or absence of FGF2. Finally, 5'-deletion of nucleotides  $-75$  to  $-51$ , encompassing the AP1 site at nucleotides  $-72$  to  $-66$  (15), substantially decreases basal promoter activity, and PE1 and FGF2 have little effect on the minimal promoter activity of 50 MMPLUC ( $-50$  to  $+63$ ). (B) PE1 suppression of the MMP1 promoter fragment  $-123$  to  $-61$  linked to the heterologous RSV basal promoter. Consistent with the 5'-deletion analyses that map PE1 repression to nucleotides  $-71$  to  $-51$  in the MMP1 promoter in panel A, transient expression of PE1 markedly suppresses basal transcription driven by MMP( $-123$  to  $-61$ ) RSVLUC. By contrast, PE1 exerts little effect on transcription driven by the RSV basal promoter (RSVLUC). See text for details.

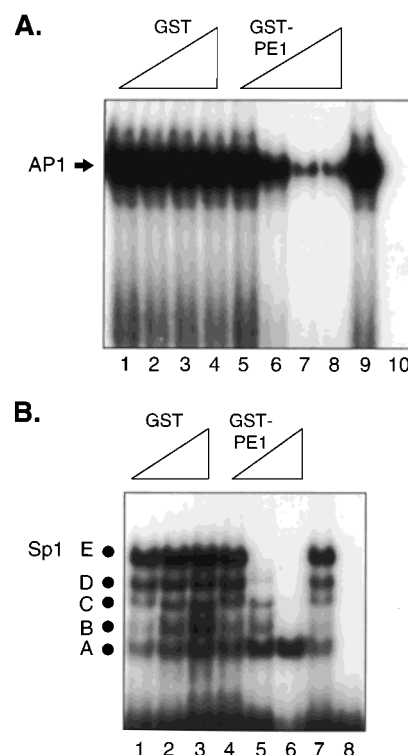


**FIGURE 7:** PE1 inhibits formation of specific protein-protein interactions at the MMP1 AP1 cognate. Crude nuclear extracts were prepared from FGF2-treated MC3T3E1 calvarial osteoblasts. The effects of recombinant GST and GST-PE1 on protein-DNA interactions at the MMP1 AP1 cognate (panel A) and a generic Sp1 cognate (panel B) were assessed by gel shift assay as detailed under Experimental Procedures. By immunologic supershift analyses, we previously demonstrated that the AP1 protein complexes assembled on the MMP1 promoter in FGF2-treated MC3T3E1 crude nuclear extracts contain Fra1 and c-Jun (15). (A) Recombinant purified GST has no effect on formation of AP1 protein-DNA complexes (lanes 1–4); by contrast, GST-PE1 suppresses AP1 binding activity (lanes 5–8). Even though GST-PE1 readily binds the Ets cognate (see Figure 4), it does not directly interact with the AP1 cognate in gel shift assay (lane 10), indicating that this inhibition occurs via PE1 protein-protein interactions. (B) In these same nuclear extracts, five complexes are identified that assemble on a Sp1 DNA binding cognate (lane 1, complexes A–E). Again, GST does not diminish the formation of these five DNA binding complexes (lanes 1–3); by contrast, while GST-PE1 decreased the binding of four of these complexes (lanes 4–6, complexes B, C, D, and E), it actually augments the formation of one DNA-protein complex assembled by the Sp1 cognate (lanes 4–6, complex A). GST-PE1 does not bind the Sp1 cognate in gel shift assay (lane 8). See text for details.

at the AP1 cognate are of prime importance for supporting MMP1 promoter activity (15, 57, 58). On this basis and the results obtained with the FGF2-stimulated, AP1-dependent proximal MMP1 promoter (75 MMPLUC, Figure 6), we surmised that PE1 must suppress the MMP1 promoter in part by antagonizing promoter activation via the AP1 element. To test this notion, we examined the effects of recombinant purified GST-PE1 on the assembly of protein-DNA complexes at the MMP1 AP1 cognate in gel shift assay, using crude nuclear extracts from FGF2-treated MC3T3E1 cells as a source of AP1 binding activity (15). As shown in Figure 7, recombinant purified GST has no effect on formation of AP1 protein-DNA complexes (Figure 7A, lanes 1–4). By contrast, GST-PE1 markedly inhibits AP1 binding activity in a dose-dependent fashion (Figure 7A, lanes 5–8). Even though GST-PE1 readily binds the Ets cognate (Figure 4,

above), it does not directly interact with the AP1 cognate in gel shift assay (Figure 7A, lane 10), indicating that it must function via protein–protein interactions. Of note, all experiments were carried out in the presence of excess BSA (BSA: GST–PE1 ratio ~200:1), indicating that the effects of PE1 on AP1 binding activity are not due to nonspecific inhibitory effects of protein on DNA binding activity. In these same MC3T3E1 nuclear extracts, 5 complexes assemble on the Sp1 DNA binding cognate (Figure 7B, lane 1, complexes A–E). Again, GST does not diminish the formation of these five DNA binding complexes (Figure 7B, lanes 1–3). By contrast, while GST–PE1 perturbs four of these complexes with differential potency (Figure 7B, lanes 4–6, complexes B–E), it does not decrease (weakly augments) the formation of a fifth protein–DNA complex assembled on the Sp1 cognate (Figure 7B, lanes 4–6, complex A). GST–PE1 does not bind the Sp1 cognate in gel shift assay (Figure 7B, lane 8), indicating that modulation of complex formation occurs via PE1 protein–protein interactions. Thus, PE1 negatively regulates DNA–protein interactions at the MMP1 promoter AP1 cognate. Suppression of DNA binding by PE1 is selective, since the “dose-dependent” downregulation of heterologous DNA binding activities by recombinant GST–PE1 is complex-specific.

## DISCUSSION

The molecular details of Ets-dependent gene transcription are only beginning to be elucidated (4, 8). In every detailed analysis to date, cooperative interactions between the Ets factor and a second, more potent transcriptional activator are necessary for transcriptional activation by the Ets protein (1, 8). For the prototypic Ets family members, Ets1 and Ets2, the transcriptional activation function maps to N-terminal domain residues far upstream of the C-terminal DNA binding Ets domain (2, 3). These residues are necessary for protein–protein interactions and recruitment of CBP/p300, transcriptional platform proteins that also bind AP1 (59). Although these platform proteins possess histone acetyltransferase (HAT) activity that remodels chromatin (3), N- and C-terminal regions of CBP that lack HAT activity appear adequate to promote Ets-dependent transcription (2). Other Ets activators also function via recruitment of CBP/p300 (4, 60); whether HAT activity is required has yet to be established. Additionally, the SUR2/DRIP130/CRSP130 subunit of the novel mammalian Srb/Med/DRIP coactivator complex (61) has been identified as interacting with the Elk1 Ets transactivation domain (62, 63). Importantly, however, the N-terminal transactivation domain present in these prototypic Ets transactivators that is required for coactivator recruitment (2, 3, 62) is absent in the Ets repressors ERF (40) and PE1 (this paper).

Little is known of the molecular mechanisms whereby Ets repressors downregulate transcription. The best-characterized protein to date is ERF (40, 64, 65). ERF constitutively represses the Ets2 promoter via a promoter-proximal Ets cognate (40). Human ERF repressor function is negatively regulated by a Ras-initiated MAPK cascade that phosphorylates Thr-526 in the C-terminus (40). Thr-526 phosphorylation of ERF directs the rapid export of the phosphoprotein from the nucleus to the cytoplasm, antagonizing ERF transcriptional suppressor function (65). Thus, Ras potentially activates ERF-regulated expression in part via transcriptional

derepression (65), similar to our evolving model of MMP1 promoter regulation by FGF2 (15).

We present for the first time the predicted full-length PE1 protein sequence, verify protein size and predicted nuclear localization in osteoblasts, and demonstrate that PE1 is a sequence-specific DNA binding protein that recognizes authentic Ets cognates present in the OPN and MMP1 promoters. We identify that PE1 is in fact a promoter-specific transcriptional suppressor, as predicted by its homology to ERF. PE1 suppresses basal MMP1 promoter activity by 50–60% but has little effect on transcription driven by the RSV promoter. Similarly, PE1 suppresses the basal OPN promoter but does not regulate the osteocalcin promoter (not shown). Our studies of PE1 point to an important role for protein–protein interactions for Ets-dependent repression. Remarkably, mPE1 does not require the Ets cognates to suppress the MMP1 promoter. Rather, PE1 usurps AP1 protein–DNA interactions that support MMP1 promoter activity in osteoblasts. Mechanistically, this model closely resembles that evolving for transcriptional repressors such as Msx2 (66) and YY1 (67). Like the homeodomain repressor Msx2, PE1 is rich in proline. Moreover, homeodomain proteins and Ets proteins are members of a larger structural class of helix–turn–helix DNA binding proteins (68, 69), a fact that may suggest similar mechanisms of transcriptional regulation. Interestingly, although largely dependent upon promoter activity driven by the bipartite Ets–AP1 motif, PE1 weakly decreases transcription directed by the minimal MMP1 (–50 to +68) and RSV (–51 to +35) promoters—driven only TATA box and Inr elements. This suggests that PE1 may interact with components of the preinitiation complex (56) and additionally usurp the interactions of transactivators with the basal machinery. Indeed, Msx2 and YY1, prototypic transcriptional repressors, suppress transcription by decreasing the binding activities of supportive transactivators (66, 67) and by targeting general transcription factors of the preinitiation complex (48, 67). However, unlike Msx2 (46, 48), PE1 does not repress OC promoter activity, and the specific protein–protein and protein–DNA interactions negatively regulated by these two repressors must be distinct. Of note, while this work was being completed it was published that ERF repression of the prolactin promoter occurs in part via inhibition of Pit1 binding to its cognate (44). Thus, both PE1 and ERF repress transcription at least in part by usurping the DNA binding activities of transactivators that support gene expression.

Cheung and co-workers (43) recently identified that the tumor suppressor p53 markedly suppresses MMP1 via the proximal promoter region we identify as being regulated by PE1. As we observe, they described that MMP1 promoter suppression by p53 is independent of a p53 cis element; rather, p53-dependent repression is achieved at least in part by secondary downregulation of AP1-dependent promoter activity. Previously, others have demonstrated that protein–protein interactions between the glucocorticoid receptor and AP1 downregulate MMP1 promoter activity (21, 70). Thus, our data demonstrating that PE1 suppresses the MMP1 promoter via perturbation of protein–DNA interactions at the AP1 cognate adds to the increasing evidence that negative regulation of this important matrix metalloproteinase occurs largely via the regulation of AP1 activity (21, 57). Recently, Shemshedini and co-workers (42) have expanded upon the

known inhibition of AP1-dependent promoters by RAR- $\alpha$  (71); they demonstrated that RAR- $\alpha$  does not merely sequester the AP1 complex but in fact disrupts Fos–Jun dimerization necessary for AP1 DNA binding activity (42). Future experiments will test whether PE1 inhibits AP1 DNA binding activity via a mechanism similar to that of the glucocorticoid receptor—i.e., by sequestering the AP1 dimeric complex (21)—or via negative regulation of Fos–Jun dimerization (21).

The precise relationships between PE1 and transcriptional regulation by FGF2 remain unclear. Murine PE1 completely lacks the Thr phosphorylation site present in ERF that mediates derepression by Ras (65). Applying both biochemical fractionation and immunofluorescence techniques, Le Gallic et al. (65) demonstrated that MAPK activation results in the nuclear export of ERF to the cytoplasm. FGF2 treatment does activate the MAPK cascade in MC3T3E1 osteoblasts (15), but unlike ERF-dependent gene regulation (65), MMP1 promoter regulation by FGF2 in MC3T3E1 cells is insensitive to MAPK cascade inhibition with PD98059 (15). Moreover, by biochemical fractionation, we observe no decrement or redistribution of nuclear 66 kDa PE1 protein upon treatment of MC3T3E1 cells with FGF2, and FGF2 treatment does not prevent PE1 suppression of the MMP1 promoter. Although the 30 kDa immunoreactive protein recognized by anti-PE1 that accumulates with FGF2 treatment potentially represents a product of regulated proteolysis, this has yet to be examined. In toto, consistent with the distinct C-terminal domains of PE1 and ERF1, our data suggest that the repressor activity of PE1 in MC3T3E1 osteoblasts is largely constitutive and is not regulated by the MAPK signaling mechanism that controls ERF activity (40, 65). Since upregulation of the MMP1 promoter by FGF2 depends on the Ets–AP1 element (15), we hypothesize that an as yet unspecified osteoblast Ets transactivator must reciprocally coregulate the MMP1 promoter in concert with PE1; MMP1 promoter activation by an FGF2-regulated osteoblast Ets transactivator would be achieved via Ets-dependent assembly of active complexes on the bipartite Ets–AP1 element, thus reversing constitutive PE1-dependent repression. Future experiments will examine whether PE1 repressor function is antagonized by Ets transactivators such as Ets2 or Erg (72) that selectively regulate the MMP1 promoter (73) and are expressed in skeletal tissues (74) that express the MMP1 gene (28, 32, 34–36, 75).

## ACKNOWLEDGMENT

We thank Dr. R. Hromas for his generous gift of the rat PE1 cDNA template.

## REFERENCES

1. Crepieux, P., Coll, J., and Stehelin, D. (1994) *Crit. Rev. Oncog.* 5, 615–38.
2. Jayaraman, G., Srinivas, R., Duggan, C., Ferreira, E., Swaminathan, S., Somasundaram, K., Williams, J., Hauser, C., Kurkinen, M., Dhar, R., Weitzman, S., Buttice, G., and Thimmapaya, B. (1999) *J. Biol. Chem.* 274, 17342–52.
3. Yang, C., Shapiro, L. H., Rivera, M., Kumar, A., and Brindle, P. K. (1998) *Mol. Cell. Biol.* 18, 2218–29.
4. Ramirez, S., Ait-Si-Ali, S., Robin, P., Trouche, D., Harel-Bellan, A., and Ait Si Ali, S. (1997) *J. Biol. Chem.* 272, 31016–21.
5. Nuchprayoon, I., Simkevich, C. P., Luo, M., Friedman, A. D., and Rosmarin, A. G. (1997) *Blood* 89, 4546–54.
6. Ratajczak, M. Z., Perrotti, D., Melotti, P., Powzaniuk, M., Calabretta, B., Onodera, K., Kregenow, D. A., Machalinski, B., and Gewirtz, A. M. (1998) *Blood* 91, 1934–46.
7. Clarke, S., and Gordon, S. (1998) *J. Leukoc. Biol.* 63, 153–68.
8. Wasyluk, B., Hagman, J., and Gutierrez-Hartmann, A. (1998) *Trends Biochem. Sci.* 23, 213–6.
9. Wang, C. Y., Petryniak, B., Thompson, C. B., Kaelin, W. G., and Leiden, J. M. (1993) *Science* 260, 1330–5.
10. Shirasaki, F., Makhluif, H. A., LeRoy, C., Watson, D. K., and Trojanowska, M. (1999) *Oncogene* 18, 7755–64.
11. Mao, S., Frank, R. C., Zhang, J., Miyazaki, Y., and Nimer, S. D. (1999) *Mol. Cell. Biol.* 19, 3635–44.
12. Zhang, D. E., Hohaus, S., Voso, M. T., Chen, H. M., Smith, L. T., Hetherington, C. J., and Tenen, D. G. (1996) *Curr. Top. Microbiol. Immunol.* 211, 137–47.
13. Sato, M., Morii, E., Komori, T., Kawahata, H., Sugimoto, M., Terai, K., Shimizu, H., Yasui, T., Ogihara, H., Yasui, N., Ochi, T., Kitamura, Y., Ito, Y., and Nomura, S. (1998) *Oncogene* 17, 1517–25.
14. Schweppe, R. E., Frazer-Abel, A. A., Gutierrez-Hartmann, A., and Bradford, A. P. (1997) *J. Biol. Chem.* 272, 30852–9.
15. Newberry, E. P., Willis, D., Latifi, T., Boudreaux, J. M., and Towler, D. A. (1997) *Mol. Endocrinol.* 11, 1129–44.
16. Pereira, R., Quang, C. T., Lesault, I., Dolznig, H., Beug, H., and Ghysdael, J. (1999) *Oncogene* 18, 1597–608.
17. Jovinge, S., Hultgardh-Nilsson, A., Regnstrom, J., and Nilsson, J. (1997) *Arterioscler. Thromb. Vasc. Biol.* 17, 490–7.
18. Celada, A., Borrás, F. E., Soler, C., Lloberas, J., Klemsz, M., van Beveren, C., McKercher, S., and Maki, R. A. (1996) *J. Exp. Med.* 184, 61–9.
19. Schneikert, J., Peterziel, H., Defosse, P. A., Klocker, H., Launoit, Y., and Cato, A. C. (1996) *J. Biol. Chem.* 271, 23907–13.
20. Klocker, H., Culig, Z., Eder, I. E., Nessler-Menardi, C., Hobisch, A., Putz, T., Bartsch, G., Peterziel, H., and Cato, A. C. (1999) *Eur. Urol.* 35, 413–9.
21. Schroen, D. J., and Brinckerhoff, C. E. (1996) *Gene Expression* 6, 197–207.
22. Tondravi, M. M., McKercher, S. R., Anderson, K., Erdmann, J. M., Quiroz, M., Maki, R., and Teitelbaum, S. L. (1997) *Nature* 386, 81–4.
23. Teitelbaum, S. L., Tondravi, M. M., and Ross, F. P. (1997) *J. Leukoc. Biol.* 61, 381–8.
24. Hernandez-Munain, C., Roberts, J. L., and Krangel, M. S. (1998) *Mol. Cell. Biol.* 18, 3223–33.
25. Westermarck, J., and Kahari, V. M. (1999) *FASEB J.* 13, 781–92.
26. Vincenti, M. P., Coon, C. I., Mengshol, J. A., Yocum, S., Mitchell, P., and Brinckerhoff, C. E. (1998) *Biochem. J.* 331, 341–6.
27. Porte, D., Tuckermann, J., Becker, M., Baumann, B., Teurich, S., Higgins, T., Owen, M. J., Schorpp-Kistner, M., and Angel, P. (1999) *Oncogene* 18, 667–78.
28. Huebner, J. L., Otterness, I. G., Freund, E. M., Caterson, B., and Kraus, V. B. (1998) *Arthritis Rheum.* 41, 877–90.
29. Tyagi, S. C., Kumar, S., Cassatt, S., and Parker, J. L. (1996) *Can. J. Physiol. Pharmacol.* 74, 983–95.
30. Coker, M. L., Thomas, C. V., Clair, M. J., Hendrick, J. W., Krombach, R. S., Galis, Z. S., and Spinale, F. G. (1998) *Am. J. Physiol.* 274, H1516–23.
31. Blankenship, T. N., and Enders, A. C. (1997) *Acta Anat.* 158, 227–36.
32. Shlopov, B. V., Lie, W. R., Mainardi, C. L., Cole, A. A., Chubinskaya, S., and Hasty, K. A. (1997) *Arthritis Rheum.* 40, 2065–74.
33. Raisz, L. G. (1999) *Clin. Chem.* 45, 1353–8.
34. Fernandes, J. C., Martel-Pelletier, J., Lascau-Coman, V., Moldovan, F., Jovanovic, D., Raynauld, J. P., and Pelletier, J. P. (1998) *J. Rheumatol.* 25, 1585–94.
35. Bord, S., Horner, A., Hembry, R. M., Reynolds, J. J., and Compston, J. E. (1997) *J. Anat.* 191, 39–48.



36. Rubin, C., Sun, Y. Q., Hadjiargyrou, M., and McLeod, K. (1999) *J. Orthoped. Res.* 17, 354–61.
37. Hurley, M. M., Tetradis, S., Huang, Y. F., Hock, J., Kream, B. E., Raisz, L. G., and Sabbieti, M. G. (1999) *J. Bone Miner. Res.* 14, 776–83.
38. Sabbieti, M. G., Marchetti, L., Abreu, C., Montero, A., Hand, A. R., Raisz, L. G., and Hurley, M. M. (1999) *Endocrinology* 140, 434–44.
39. Hurley, M. M., Marcello, K., Abreu, C., Brinckerhoff, C. E., Bowik, C. C., and Hibbs, M. S. (1995) *Biochem. Biophys. Res. Commun.* 214, 331–9.
40. Sgouras, D. N., Athanasiou, M. A., Beal, G. J., Jr., Fisher, R. J., Blair, D. G., and Mavrothalassitis, G. J. (1995) *EMBO J.* 14, 4781–93.
41. Klemsz, M., Hromas, R., Raskind, W., Bruno, E., and Hoffman, R. (1994) *Genomics* 20, 291–4.
42. Zhou, X. F., Shen, X. Q., and Shemshedini, L. (1999) *Mol. Endocrinol.* 13, 276–85.
43. Sun, Y., Wenger, L., Rutter, J. L., Brinckerhoff, C. E., and Cheung, H. S. (1999) *Ann. N.Y. Acad. Sci.* 878, 638–41.
44. Day, R. N., Liu, J., Sundmark, V., Kaweck, M., Berry, D., and Elsholtz, H. P. (1998) *J. Biol. Chem.* 273, 31909–15.
45. Boudreaux, J. M., and Towler, D. A. (1996) *J. Biol. Chem.* 271, 7508–15.
46. Towler, D. A., Rutledge, S. J., and Rodan, G. A. (1994) *Mol. Endocrinol.* 8, 1484–93.
47. Lane, D., and Harlow, E. (1988) *Antibodies: a laboratory manual*, Cold Spring Harbor Laboratory, Cold Spring Harbor, NY.
48. Newberry, E. P., Latifi, T., Battaile, J. T., and Towler, D. A. (1997) *Biochemistry* 36, 10451–62.
49. Dignam, J. D., Lebovitz, R. M., and Roeder, R. G. (1983) *Nucleic Acids Res.* 11, 1475–89.
50. Peterson, G. L. (1977) *Anal. Biochem.* 83, 346–56.
51. Margolis, R. L., and Wilson, L. (1998) *Bioessays* 20, 830–6.
52. Warburton, P. E., and Earnshaw, W. C. (1997) *Bioessays* 19, 97–9.
53. Towler, D. A., Bennett, C. D., and Rodan, G. A. (1994) *Mol. Endocrinol.* 8, 614–24.
54. Towler, D. A., and Rodan, G. A. (1995) *Endocrinology* 136, 1089–96.
55. Kozak, M. (1992) *Annu. Rev. Cell Biol.* 8, 197–225.
56. Green, M. R. (2000) *Trends Biochem. Sci.* 25, 59–63.
57. Borden, P., and Heller, R. A. (1997) *Crit. Rev. Eukaryotic Gene Expression* 7, 159–78.
58. Chapman, S. C., Ayala, J. E., Streeper, R. S., Culbert, A. A., Eaton, E. M., Svitek, C. A., Goldman, J. K., Tavar, J. M., and O'Brien, R. M. (1999) *J. Biol. Chem.* 274, 18625–34.
59. Korzus, E., Torchia, J., Rose, D. W., Xu, L., Kurokawa, R., McInerney, E. M., Mullen, T. M., Glass, C. K., and Rosenfeld, M. G. (1998) *Science* 279, 703–7.
60. Yamamoto, H., Kihara-Negishi, F., Yamada, T., Hashimoto, Y., and Oikawa, T. (1999) *Oncogene* 18, 1495–501.
61. Freedman, L. P. (1999) *Cell* 97, 5–8.
62. Boyer, T. G., Martin, M. E., Lees, E., Ricciardi, R. P., and Berk, A. J. (1999) *Nature* 399, 276–9.
63. Rachez, C., Lemon, B. D., Suldan, Z., Bromleigh, V., Gamble, M., Naar, A. M., Erdjument-Bromage, H., Tempst, P., and Freedman, L. P. (1999) *Nature* 398, 824–8.
64. Liu, D., Pavlopoulos, E., Modi, W., Moschonas, N., and Mavrothalassitis, G. (1997) *Oncogene* 14, 1445–51.
65. Le Gallic, L., Sgouras, D., Beal, G. J., Jr., and Mavrothalassitis, G. (1999) *Mol. Cell. Biol.* 19, 4121–33.
66. Newberry, E. P., Boudreaux, J. M., and Towler, D. A. (1997) *J. Biol. Chem.* 272, 29607–13.
67. Guo, B., Aslam, F., van Wijnen, A. J., Roberts, S. G., Frenkel, B., Green, M. R., DeLuca, H., Lian, J. B., Stein, G. S., and Stein, J. L. (1997) *Proc. Natl. Acad. Sci. U.S.A.* 94, 121–6.
68. Kohn, W. D., Mant, C. T., and Hodges, R. S. (1997) *J. Biol. Chem.* 272, 2583–6.
69. Pio, F., Kodandapani, R., Ni, C. Z., Shepard, W., Klemsz, M., McKercher, S. R., Maki, R. A., and Ely, K. R. (1996) *J. Biol. Chem.* 271, 23329–37.
70. Reichardt, H. M., Kaestner, K. H., Tuckermann, J., Kretz, O., Wessely, O., Bock, R., Gass, P., Schmid, W., Herrlich, P., Angel, P., and Schutz, G. (1998) *Cell* 93, 531–41.
71. Chen, J. Y., Penco, S., Ostrowski, J., Balaguer, P., Pons, M., Starrett, J. E., Reczek, P., Chambon, P., and Gronemeyer, H. (1995) *EMBO J.* 14, 1187–97.
72. Basuyaux, J. P., Ferreira, E., Stehelin, D., and Buttice, G. (1997) *J. Biol. Chem.* 272, 26188–95.
73. Buttice, G., Duterte-Coquillaud, M., Basuyaux, J. P., Carrere, S., Kurkinen, M., and Stehelin, D. (1996) *Oncogene* 13, 2297–306.
74. Dhordain, P., Dewitte, F., Desbiens, X., Stehelin, D., and Duterte-Coquillaud, M. (1995) *Mech. Dev.* 50, 17–28.
75. Freemont, A. J., Hampson, V., Tilman, R., Goupille, P., Taiwo, Y., and Hoyland, J. A. (1997) *Ann. Rheum. Dis.* 56, 542–9.

BI000343+